Is Nonlinear Analysis Becoming a Standard Tool for Design and Assessment of Reinforced Concrete Structures?

Jan Červenka, Jiří Rymeš, Libor Jendele, and Radomír Pukl

Červenka Consulting s.r.o. Prague, Czech Republic

Contact: jan.cervenka@cervenka.cz

Abstract

The nonlinear finite element method has become a standard tool serving engineers during the designing of reinforced concrete bridges. Compared to a linear solution, the main advantage is that it can provide a better insight into the realistic material response including crack formation and subsequent redistribution of internal forces. In this paper, the key aspects related to the application in engineering practice are summarised, including the theory behind the nonlinear material model and the explanation of the solution method. Based on validation against experimental data, the accuracy of a given nonlinear tool can be quantified and translated into a model partial safety factor. This factor then serves as a parameter in the evaluation of the design structural resistance. Finally, we show an example of an assessment of a post-tensioned reinforced concrete bridge, where strengthening provisions were adopted to reinforce a critical region with crack formation.

Keywords: finite element analysis, reinforced concrete structures, nonlinear simulation, damage mechanics, smeared crack models, reliability analysis.

1 Introduction

Application of the nonlinear finite element method (FEM) during the designing of reinforced concrete structures offers engineers an important perspective into the realistic behavior of the structure. Advanced material models can evaluate the crushing of concrete when subjected to high compressive stress as well as cracking when the tensile strength is exceeded. Furthermore, for the reinforcement material, yielding and even rupturing can be simulated. By these means, a complex assessment of the structural performance is feasible. Compare to traditional design approaches based on the classic beam theory, nonlinear FEM can accurately consider complex geometries, stress states, and loading histories. This allows assessment of the structural integrity for static, dynamic, and environmental loads as well as consideration of the long-term rheological phenomena such as concrete creep.

The applicability of the nonlinear FEM simulation has been rigorously shown in literature and is often checked in benchmark competitions. Based on these findings, modeling uncertainties can be quantified. To utilize nonlinear analysis in engineering practice, proper guidelines need to be available. Currently, these provisions are given in the *fib* Model Code 2010 [1] and will be introduced in the new generation of Eurocodes. These standards incorporate the model uncertainty, which should be specific to each material model and software package.

This paper is structured to first give a brief theoretical overview of the non-linear FEM, demonstrate its applicability using examples from benchmark competitions, and finally present a code-based framework for engineering application.

The second part of the paper then shows an example of the analysis, where the nonlinear analysis was used to assess the crack width in the structure of a post-tensioned reinforced concrete bridge.

2 Nonlinear analysis overview

Before presenting the example of application, the framework for nonlinear analysis is described. We briefly cover the theory, show validation against experimental data, and explain the uncertainties in the modeling and the safety format for the application of the nonlinear FEM in engineering practice.

2.1 Fracture-plastic model with smeared cracks

The essential part of the nonlinear simulations is the availability of material models that can realistically describe the actual material performance. In the field of material science, this is most commonly represented by a stress-strain diagram. On top of that, the material laws should respect physics principles. When talking about concrete, these are typically used as additional criteria for describing the nonlinear response, for example in terms of fracture energy dissipated for crack propagation or volumetric variation during concrete crushing.

The data for this paper were collected using the ATENA software package, which implements the fracture-plastic model proposed by Červenka J. et al. [2,3]. It divides the nonlinear material response in tension and compression.

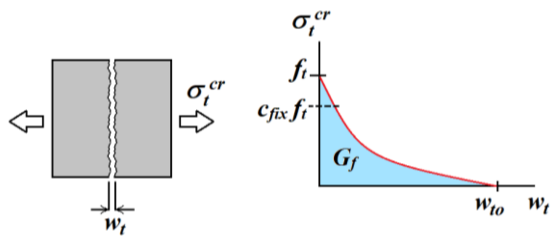

Figure 1. The fracture crack opening law that controls the softening response in tension.

The tensile post-peak response is characterized by an orthotropic smeared crack model with a softening curve controlled by the fracture energy that is dissipated during the crack propagation as shown in Figure 1. The fracture process is simulated using the so-called smeared crack approach. Rather than explicitly tracking each individual crack, the smeared crack approach adds the response of multiple cracks within a single element and adequately reduces the strength of the element. The cracking model is orthotropic and allows the formation of up to three cracks in the three principal directions.

It has been observed that the smeared crack models suffer certain mesh dependency. For instance, if large elements in order of hundreds of millimeters or even meters are used in the model, the assumption that a single crack develops in a principle tension direction is no longer valid. In reality, several cracks form in the case of a reinforced concrete sample. Therefore, the total fracture energy available for dissipation is underestimated in the simulation thus reducing the peak load. This can be adjusted by an additional material parameter specifying the crack spacing [4]. Analogically, if a very small mesh is used, the number of cracks may be overestimated. In reality, the minimum crack spacing would be limited by the internal material length scale depending on the aggregate size [4]. By imposing a limit on minimum crack spacing distance, it can be ensured that the crack will localize in a physically plausible distance range.

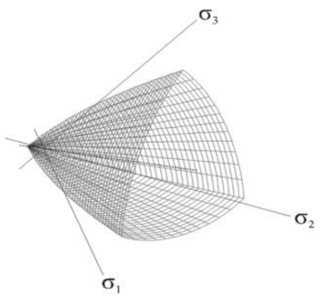

Figure 2. Menetrey & Willam failure criterion [5].

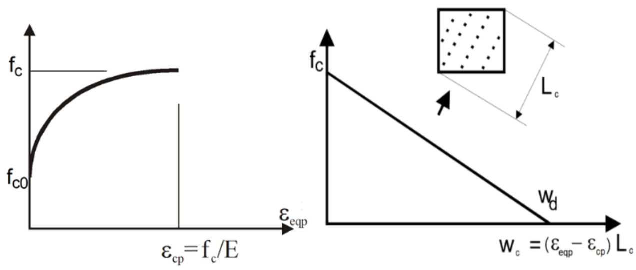

Figure 3. Hardening/softening law for the plasticity model for concrete in compression.

The compression branch is described by the plasticity approach with the Menetrey & Willam failure criterion [5] shown in Figure 2. As shown in Figure 3, hardening is modeled after exceeding the stress level corresponding to the onset of crushing with linear softening after reaching the compressive strength. The material model incorporates a yield surface and flow rule to capture the compressive plasticity of the material.

When nonlinear material laws are introduced into the FEM, the set of equations to be solved becomes nonlinear. Therefore, a suitable solver technique is necessary to find the equilibrium between the nodal displacement and material response. This is called the convergence of the solution. Most commonly, these methods are derived from the well-known Newton-Raphson method. The iterative solution runs until the residual error decreases below the prescribed convergence criteria. It is needless to say that only the results, where the convergence of the solution was reached, should be used for structural analysis. The loss of convergence is sometimes an indicator that the ultimate load-bearing capacity was exceeded; however, the results should be always carefully inspected to determine the actual cause of divergence.

Once the convergence at a given load step is obtained, the next load step is calculated based on the previously calculated state. Unlike in the linear (i.e., elastic) solution, the superposition principle is not valid, meaning that the structural response under multiple loadings cannot be found by simple addition. Therefore, the loading history plays an important role in the simulation and should resemble the actual loading scenario.

Most engineering applications are formulated as load-prescribed tasks since the design standards generally specify the external loads. For this purpose, the arc-length method [6,7] is more suitable as it scales the load vector based on the displacement increment, and thus is capable to automatically scale or even decrease the applied load when maximum load-carrying capacity is reached. This allows for obtaining a realistic load-displacement diagram describing the global response of the model, including the post-peak behavior.

2.2 Validation and benchmark predictions

To ensure the applicability of the above-described theory in practical design or assessment of existing reinforced concrete structures, the nonlinear numerical tools are validated against experimental data. Such tests can be generally divided into two groups of data.

In the first case, a numerical model is used for reproducing a laboratory experiment to provide a better insight into certain aspects of the specimen's behavior. For such data, there is always a possibility that the author adjusted some of the default parameters of the material model, the solution criteria, or re-modeled part of the set-up to get a better match with the experimental results. Such a procedure is admissible when the existing material models are fitted to a new material with ambiguous response; however, is not suited for validation of the nonlinear FEM framework for well-known materials.

The second type of validation can be provided by blind predictions. These contests often aim at the simulation of failure mechanisms that are still not fully understood. For instance, the bending failure can be simulated with better confidence that the shear or punching failure mechanism. Similarly, blind tests are conducted also for new materials such as fiber-reinforced concrete.

As an example, two blind predictions, that were designed to investigate the shear failure mechanism, are described here (for more examples see reference [8]). The geometry of the specimen tested at the blind prediction organized by Collins et al. [9] is shown in Figure 4 and the sample tested by the UC Berkley group [10] is shown in Figure 5. Both specimens were designed similarly when one half was without shear reinforcement while the opposite half was reinforced with stirrups. During the loading, the shear failure first naturally occurred in the unreinforced half, which was subsequently constrained to allow the load to be increased until the shear failure also developed at the reinforced half of the beam. Therefore, a single specimen was used to obtain two test results in both competitions.

The comparison between the load-displacement curve obtained in the experiments and from the

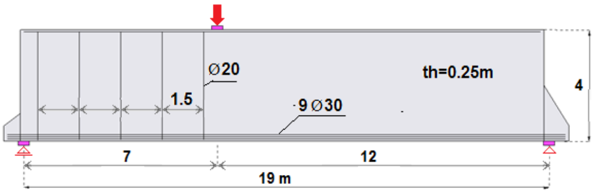

Figure 4 Schematic of the deep beam tested by Collins et al. [9].

numerical simulation is shown in Figure 6 for the experiment by Collins and in Figure 7 for the experiment conducted at US Berkeley, respectively. As is evident from Figure 6, the submitted prediction realistically estimated the response. As a matter of fact, these results were awarded as the winning prediction.

On the other hand, the initial simulation of the experiment at US Berkeley significantly underestimated the actual strength. Especially for the test without stirrups, the peak load was underestimated almost by 50 % (labeled as Sim. 1) and even if accounted for the self-weight of the specimen (515 kN), there was still approximately 25 % and 22 % difference for the half of the beam with and without shear reinforcement, respectively.

The main source of inaccuracy in the simulation was the application of the shrinkage strain of -150 µ. If not applied, the error of the analysis was reduced to 25 %, or 12 % considering the self-weight (labeled as Sim. 1 default).

Furthermore, when simulating the shear failure mechanism, an important role plays the cracked concrete shear stiffness factor that controls the shear stiffness of the material, where a crack has

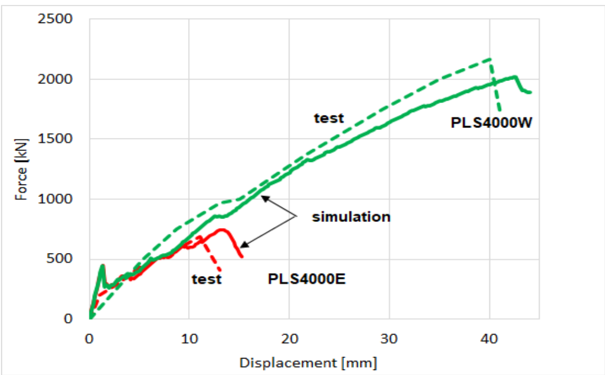

Figure 6 Comparison of the load-displacement diagrams from the experiment and simulation for the competition by Collins et al.

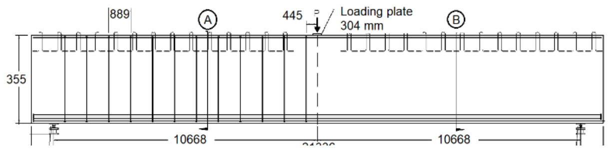

formed. The default value used in the discussed material model is 20. If its value is increased to 100 (labeled as Sim. 1, default, sF 100), the match with the experiment can be improved. For the sake of comparison, in the winning prediction in the benchmark organized by Collins, a shear stiffness factor of 50 was used.

Figure 5 Geometry of the specimen tested at UC Berkeley competition [10].

It should also be noted that only one sample was tested at each competition so the comparison here is inevitably affected by the lack of statistical data. Considering material heterogeneity typical for concrete, a wider data set would be favorable to draw better conclusions. From this point, setting the shear stiffness factor to 20 can be seen as a conservative design approach.

2.3 Model uncertainties and safety factors

Model uncertainty refers to the ratio between the resistance found experimentally R_{exp} and the resistance obtained in the simulation R_{sim}. This can be written as:

$$\theta = \frac{R_{exp}}{R_{sim}} \quad . \qquad (1)$$

It is assumed that it is a random variable that should be obtained by statistical evaluation of a set of data. Assuming the lognormal distribution of the

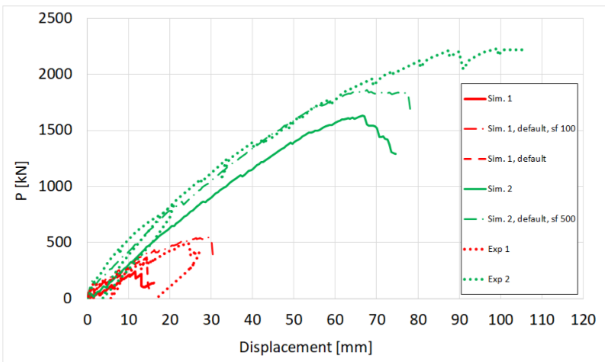

Figure 7 Comparison of the load-displacement diagrams from the experiment and simulation for the US Berkeley competition.

evaluated dataset, the safety factor for model uncertainty γ_{Rd} can be calculated as:

$$\gamma_{Rd} = \frac{\exp(\alpha_R \cdot \beta \cdot V_\theta)}{\mu_\theta} \quad , \tag{2}$$

where μ_Θ is the mean value of the model uncertainty and V_Θ is the coefficient of variation. For the sensitivity factor for the reliability of resistance α_R and the reliability index β values of 0.8 and 3.8 can be taken [11].

It should be noted that the model partial safety factor is specific to a given software package or material model. Furthermore, it can differ based on the loading mode, i.e., whether the failure at the ultimate resistance is governed by bending, shear, or compression.

For a given concrete nonlinear material model, several parameters are typically needed while the material is typically characterized only by compression test during the experiment. The remaining parameters of the material model are then deduced from the value of the compressive strength using a set of empirical equations. The uncertainty included in these equations is thus contained in the model partial safety factor.

Table 1. Partial safety factors for model uncertainty from the study of Červenka V [12].

Failure type	μ_θ	V_θ	γ_{Rd}
Punching	0.971	0.076	1.16
Shear	0.984	0.067	1.13
Bending	1.072	0.052	1.01
All failure modes	0.979	0.081	1.16

The model uncertainty was previously calculated for different models [13–16]. As this paper describes the data obtained by the ATENA software package, the study of Červenka V. et al. [12] should be mentioned here. In this study, the material model described above [2,3] was validated against the results of 33 samples failing either in punching, shear, or bending. The model partial safety factors for each failure mode are summarised in Table 1. The resulting value for all failure modes yielded 1.16. Again, it is important to bear in mind that this value is only valid for the ATENA software in combination with the model by Červenka J. [2,3]

2.4 Safety format

To apply the findings from nonlinear FEM analysis in engineering practice, an appropriate safety framework needs to be available. Currently, such guidelines are given in the *fib* Model Code [11] and a similar approach, is about to be introduced in the new generation Eurocodes.

The structural requirements specify that the design structural resistance R_d must be greater than the effect of design loads E_d. Therefore:

$$E_d < R_d \quad . \tag{3}$$

The *fib* Model Code [11] lists three kinds of nonlinear methods for obtaining the design structural resistance. These are the full probabilistic, global resistance, and partial factor methods (PFM).

The method closest to the traditional cross-section designing is the PFM. It specifies that the parameters of the concrete nonlinear material model are deduced from the design value of the concrete compressive strength. Design material parameters are adopted also for other materials in the model, such as reinforcement yield strength or rapture strain. During the analysis run, the design load combination is gradually increased until the maximum load-bearing capacity is found. The maximum load value gives the global resistance, which should be further reduced by the model partial safety factor to obtain design structural resistance.

The estimate of the coefficient of variation (ECoV) method belongs to the global resistance method group and was originally proposed by Červenka V. [17]. It assumes that the design structural resistance follows the lognormal distribution, which can be characterized by the characteristic R_k and mean structural R_m resistances. From these, the coefficient of variation V_R can be calculated:

$$V_R = \frac{1}{1.65} \ln\left(\frac{R_m}{R_k}\right) \quad . \tag{4}$$

and the global resistance factor γ_R :

$$\gamma_R = \exp(\alpha_R \, \beta \, V_R) \quad . \tag{5}$$

Finally, the design structural resistance according to the ECoV method is calculated:

$$R_{d,ECOV} = \frac{R_m}{\gamma_R \, \gamma_{Rd}} \quad . \tag{6}$$

The *fib* Model Code [11] also lists the full probabilistic method; however, it can be unlikely applied in engineering practice as it would require hundreds of analysis runs to fully describe the distribution of the structural resistance.

3 Example of application

3.1 Strengthening of box girder bridge

The application of the nonlinear FEM is demonstrated using the analysis of a viaduct in the Czech Republic. The presented analysis aimed at the assessment of the serviceability limit state of the structure in terms of crack width. Compared to the conventional structural analysis based on the beam theory, the 3D FEM allows accurate consideration of the stress state in the web. For large shear stresses, the assumption that the beam cross-section remains planar after deformation is not necessarily valid, therefore, the 3D model is advantageous. Furthermore, the nonlinear analysis also considers the redistribution of the internal forces due to cracking. A brief summary of the analysis is given here.

Figure 8. A view of the investigated viaduct.

The bridge is an integral part of the main highway connecting the Czech capital Prague with the Saxony region, Germany. From the structural viewpoint, it is a post-tensioned reinforced concrete box girder bridge with a span of 48 meters. The depth of the box girder is 2.7 meters. The bridge is shown in Figure 8. During the construction phase, diagonal cracks formed in the web of the box girder at the segments close to the pier supports. The cracks formed during a prolonged construction interruption before the placement of the road deck on the structure of the bridge.

In the simulation, a typical section of the bridge corresponding to the pier and half of the span on each side was modeled. At the midspans, the internal forces obtained from a global beam model were applied as the external load to ensure the realistic behavior of the partial model. This simulation aims at the assessment of the realistic crack state, therefore, mean material parameters were used in the material model.

The analysis considers the actual history of the structure, including the construction phase. The construction process among others simulated the balanced cantilever construction method, construction interruption, and high thermal loads during this period. The compliance function from Eurocode [18] was used for considering the long-term concrete creep. The observed crack pattern was successfully reproduced in the simulation.

In response to the shear crack formation suggesting a possible weak point, the operating authorities decided to implement strengthening measures. The strengthening should ensure that the cracks will not further propagate and enhance the overall robustness. It was designed in the form of additional post-tensioned cables placed in the box girders and anchored at steel deviators.

In Figure 9, an example of the analysis outcome is plotted. Before the strengthening, the maximum crack width in the box girder web was in the range of approximately 0.50 - 0.75 mm as shown in Figure 9 a). This crack width corresponded to the moment when the construction process was finished and the bridge was opened for traffic. After the prestressing cables were installed, the crack width decreases to approximately 0.20 - 0.40 mm. The crack width distribution after the strengthening and the stresses in the strengthening cables are shown in Figure 9 b) and c), respectively.

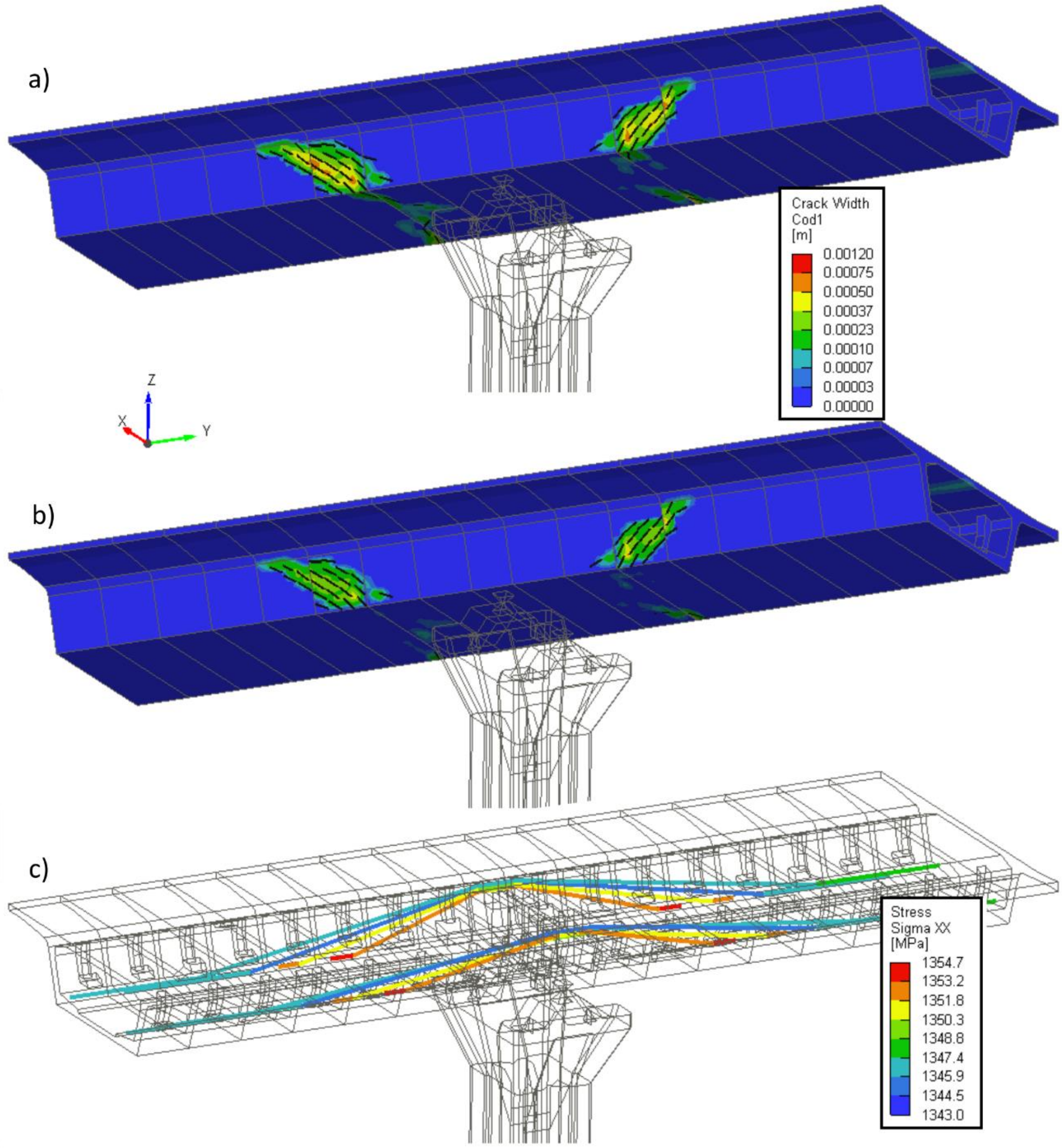

Figure 9. Results of the simulation of the viaduct strengthening: a) crack width before strengthening, b) crack width after strengthening, and c) stresses in the strengthening cables (only cracks larger than 0.1 mm are emphasized).

4 Summary

This paper presents the background for the application of nonlinear analysis for the design and assessment of reinforced concrete bridges. The core component of a nonlinear numerical simulation is the material model that can successfully simulate the performance of the real material, including the failure (i.e., post-peak) response. Currently, in the scale of typical engineering applications, the smeared crack model with a crack band is available and has been proven to accurately reproduce laboratory tests as well as blind predictions. The accuracy of a given material model and software package is described by a model uncertainty and reflected by the model safety factor.

In the second part of this paper, an application example is presented. It shows an assessment of the crack width in a pre-stressed reinforced concrete box girder bridge. The analysis successfully reproduced the cracks that developed in the structure during a prolonged construction interruption. Since it was decided that additional strengthening will be applied in the critical region subjected to cracking, the nonlinear FEM analysis was further used to evaluate how the strengthening will reduce the existing crack width.

5 Acknowledgments

The data presented in this study were obtained with the financial support of the Czech Technological Agency under the project TM04000012 “BRIHIS - A concrete bridge health interpretation system based on mutual boost of big data and physical mechanism” within the Delta 2 Programme. The financial support is greatly acknowledged.

6 References

[1] International Federation for Structural Concrete. fib Model Code for Concrete Structures 2010. 2013. 434 p.

[2] Červenka J, Červenka V, Eligehausen R. Fracture-plastic material model for concrete, application to analysis of powder actuated anchors. In: Proceedings FRAMCOS (3). 1998. p. 1107–16.

[3] Červenka J, Papanikolaou VK. Three dimensional combined fracture–plastic material model for concrete. Int J Plast. 2008 Dec 1;**24**(12):2192–220.

[4] Červenka J, Červenka V, Laserna S. On crack band model in finite element analysis of concrete fracture in engineering practice. Eng Fract Mech [Internet]. 2018;**197**:27–47.

[5] Willam PM and KJ. Triaxial Failure Criterion for Concrete and its Generalization. ACI Struct J. **92**(3).

[6] Červenka V, Jendele L, Červenka J. ATENA Program Documentation: Part 1 Theory. Prague; 2022. 360 p.

[7] Crisfield MA. An arc-length method including line searches and accelerations. Int J Numer Methods Eng [Internet]. 1983 Sep 1;**19**(9):1269–89.

[8] Červenka J, Šmejkal F, Červenka V, Kurmann D. On the application of nonlinear analysis in the design and assessment of reinforced concrete structures. In: Meschke, Pichler, Rots, editors. Computational Modelling of Concrete and Concrete Structures. CRC Press; 2022. p. 8–21.

[9] Collins MP, Bentz EC, Quach PT, Proestos GT. The challenge of predicting the shear strength of very thick slabs. Concr Int. 2015;**37**(11):29–37.

[10] Moehle J, Zhai J. Thick Foundation Element Blind Prediction Contest [Internet]. 2021. Available from: peer.berkeley.edu/news-and-events/2021-thick-foundation-element-blind-prediction-contest

[11] International Federation for Structural Concrete. fib Model Code for Concrete Structures 2010. 2013. 434 p.

[12] Červenka V, Červenka J, Kadlec L. Model uncertainties in numerical simulations of reinforced concrete structures. Struct Concr. 2018;**19**(6):2004–16.

[13] Engen M, Hendriks MAN, Köhler J, Øverli JA, Åldstedt E. A quantification of the modelling uncertainty of non-linear finite element analyses of large concrete structures. Struct Saf. 2017 Jan 1;**64**:1–8.

[14] Castaldo P, Gino D, Bertagnoli G, Mancini G. Partial safety factor for resistance model uncertainties in 2D non-linear finite element analysis of reinforced concrete structures. Eng Struct. 2018 Dec 1;**176**:746–62.

[15] Gino D, Castaldo P, Giordan L, Mancini G. Model uncertainty in non-linear numerical analyses of slender reinforced concrete members. Struct Concr. 2021;**22**:845– 870.

[16] Castaldo P, Gino D, Bertagnoli G, Mancini G. Resistance model uncertainty in non-linear finite element analyses of cyclically loaded reinforced concrete systems. Eng Struct. 2020 May 15;**211**:110496.

[17] Červenka V. Global Safety Format for Nonlinear Calculation of Rein-forced Concrete. Beton- und Stahlbetonbau. 2018;**103**:37–42.

[18] European Committee for Standardization. Eurocode 2: Design of concrete structures - Part 1-1: General rules, and rules for buildings. 2004.